INDERSCIENCE PUBLISHERS
Linking academia, business and industry through research

International Journal of Machining and Machinability of Materials

ISSN online: 1748-572X - ISSN print: 1748-5711
https://www.inderscience.com/ijmmm

Study on tearing defects in high-speed milling of aluminium honeycomb core

Hualin Zheng, Haoran Zhang, Huan Chen

DOI: 10.1504/IJMMM.2025.10068693

Article History:

Received:	06 September 2023
Last revised:	28 November 2023
Accepted:	01 December 2023
Published online:	18 March 2025

Study on tearing defects in high-speed milling of aluminium honeycomb core

Hualin Zheng*, Haoran Zhang and Huan Chen

School of Mechatronic Engineering,
Southwest Petroleum University,
Chengdu, China
Email: zhl@swpu.edu.cn
Email: 1136349275@qq.com
Email: 1442924561@qq.com
*Corresponding author

Abstract: The tearing defect generated during the processing of aluminium honeycomb core is one of the main factors to reduce the bonding strength between the aluminium honeycomb core and connective face sheet. In order to study the tearing defects formed during high-speed milling of aluminium honeycomb cores, a finite element model for cutting a single honeycomb wall was established. The influence of main processing parameters on tearing defects was explored, and the variation law between tearing defects and cutting forces under different processing parameters was further analysed. The results show that when the entrance angle is in regions I and III, the force $F_{\parallel}$ parallel to the honeycomb wall is the main reason for the formation of tearing defects. When the entrance angle is in region II, the force $F_{\perp}$ perpendicular to the honeycomb wall has a great influence on the tearing defect. The degree of tearing defects is positively correlated with the force $F_{\parallel}$ parallel to the honeycomb wall in general, and the influence on tearing defects follows that the entrance angle > feed speed > cutting speed.

Keywords: aluminium honeycomb core; finite element simulation; cutting force; tearing defect; milling parameter.

Reference to this paper should be made as follows: Zheng, H., Zhang, H. and Chen, H. (2025) 'Study on tearing defects in high-speed milling of aluminium honeycomb core', *Int. J. Machining and Machinability of Materials*, Vol. 27, No. 1, pp.4–18.

Biographical notes: Hualin Zheng is a Professor and Doctoral Supervisor at Southwest Petroleum University. His main research directions are intelligent manufacturing, difficult to machine material cutting theory and processing technology, and composite material processing theory and application. He led or participated in eight national level projects, including National Science and Technology Major Projects, National 863 Plan, National Science and Technology Support Plan, and National Natural Science Foundation of China. He published over 80 academic papers, including nearly 20 indexed by SCI and EI, and authorised nearly ten national invention patents. He has guided more than 50 Doctoral and Master's students.

Haoran Zhang is a Master's student at Southwest Petroleum University, majoring in Mechanical Engineering. His main research direction is milling technology for composite materials and micro finite element simulation of composite materials. He participated in the 'Research on processing damage

and process optimisation of Chengfei carbon fibre composite materials' project, where he was responsible for finite element analysis. During his school years, He published a patent, serving as a teaching assistant for undergraduate students.

Huan Chen is a Master's student at Southwest Petroleum University, majoring in Mechanical Engineering. Her main research direction is milling technology for composite materials and micro finite element simulation of composite materials. She is skilled in modelling software such as CAD, Soildworks, CAE, etc. During her school years, she published a patent and was awarded an academic scholarship.

1 Introduction

Aluminium honeycomb core material is a thin-walled multi-core lattice structure material. It has the characteristics of high wind pressure resistance, shock absorption and high specific strength, which has a wide range of applications in aerospace, automotive and other fields (Wang et al., 2020a). High-speed milling is one of the commonly used processing methods for aluminium honeycomb core (Zhang, 2021), due to the small thickness of honeycomb wall, the material will appear deformation, tearing, burrs and other defects during the cutting process, which seriously affects the surface quality of the workpiece (Sun et al., 2017).

At present, many scholars have carried out research on the processing defects of honeycomb materials. Wang et al. (2017).compared the ice fixation method with the conventional fixation method. The results show that ice holding can effectively improve the processing quality. Wang et al. (2020b) analysed the influence of processing parameters on surface roughness and surface morphology, and determined the optimal cutting parameters. Wang et al. (2021) analysed the influence of milling depth and ice holding height on the deformation of honeycomb wall by finite element simulation. Hamid et al. (2022) developed a specific method based on microscopic observation to analyse the surface integrity of aluminium honeycomb cores. Tarik et al. (2022a) established a 3D finite element model based on the Lagrangian method. The influence of different cutting conditions on cutting force and chip morphology was analysed by finite element model. Jaafara (2017) analysed the machinability of cutting parameters on Nomex material by numerical simulation. Jiang and Liu (2021) predicted the cutting force at different cutting angles by establishing a numerical model of the cutting force of the Nomex honeycomb core. At the same time, the finite element simulation method is used to reveal the formation mechanism of honeycomb wall tearing defects. Shi et al. (2022) carried out experiments and simulations on high-temperature alloy honeycomb cores, and analysed the effects of milling parameters, tool types and milling methods on cutting force and machining damage during millining.

The existing research shows that the tearing defect accounts for the largest proportion in the machining damage, which has the greatest influence on the application of honeycomb sandwich plate and is one of the important factors affecting the surface quality of the workpiece. It is mainly affected by processing parameters and cutting force. Among the processing parameters, cutting speed and feed speed have the greatest influence on tearing defects (Zhang, 2021). Nevertheless, there are few studies on the

factors affecting the formation of aluminium honeycomb core defects in the existing literature.

In the process of machining, due to the short contact time between the tool and the honeycomb wall, the traditional method cannot observe the process of tearing defects. The main objective of this work is to model and simulate the formation process of tearing defects in the milling process of 5052 aluminium honeycomb structure. The influence of main cutting parameters on cutting force and tearing defects is studied. Firstly, the finite element model is verified by experimental tests. Secondly, the parametric analysis is carried out, and the influence of cutting angle, feed speed and cutting speed on the tearing defect and cutting force of aluminium honeycomb core is analysed. Finally, the relationship between cutting force and tearing defects under different processing parameters is studied.

2 Finite element cutting simulation model

2.1 Finite element geometric model

Finite element simulation can effectively predict the formation of tearing defects and the trend of cutting force. In this study, the Explicit module in Abaqus is used to simulate the milling process of aluminium honeycomb core. Unlike the cutting process of traditional metal materials, the honeycomb core has a thin wall, and the cutting process between the tip of the tool and the honeycomb wall is completed in a very short time, so the cutting motion of the tool can be regarded as a straight-line motion along the direction of the cutting speed in a very short time (Qiu, 2017). In this case, the machining process is not only affected by the cutting parameters such as cutting speed and feed speed, but also the angle between the honeycomb wall and the direction of the tool's cutting speed (honeycomb wall's entrance angle θ) becomes one of the key factors. The cutting process of honeycomb core is composed of the cutting process of each honeycomb wall, and when the contact position of honeycomb wall with the tool changes, the angle of incision also changes from θ1 to θ2, as shown in Figure 1.

Figure 2 shows the 3D cutting simulation model of aluminium honeycomb core. Because the honeycomb core is a thin-walled material, the contact part of the cutting tool and the honeycomb wall is limited to the tip part, so the tool is simplified to a tip model with radial rake angle, axial rake angle and clearance angle. The honeycomb core was a square hexagonal shape with the thickness of wall was set as 0.06 mm. The cell type of the mesh used for the aluminium honeycomb core is C3D8R, and the cell type of the mesh used for the tool is C3D4, and the bottom of the honeycomb core is completely fixed. The tool is defined as a rigid body, and the tool has a radial rake angle of 15°, an axial rake angle of 30°, and a clearance angle of 35°, and the contact between tool and workpiece is universal contact. During the machining process, the friction coefficient between the tool and the aluminium honeycomb core has an important effect on the simulation results, and according to Tarik et al. (2022b), the friction coefficient was set as 0.3. The cutting width of the honeycomb wall is calculated from the feed per tooth of the tool. The simulated cutting parameters are shown in Table 1 and the material parameters are shown in Table 2.

Figure 1 Entrance angle diagram of honeycomb core (see online version for colours)

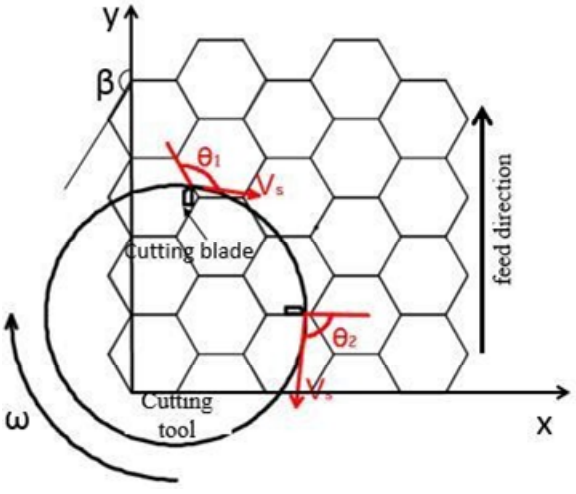

Table 1 Simulated cutting parameter

Properties	*Value*
Feed speed(mm/min)	240, 480, 720, 960
Cutting speed(m/min)	240, 320, 400
Entrance angle/°	10, 13, 30, 45, 60, 75, 90, 105, 120, 135, 150, 160, 170
Cutting depth/mm	1

Figure 2 Aluminium honeycomb core 3D cutting simulation model (see online version for colours)

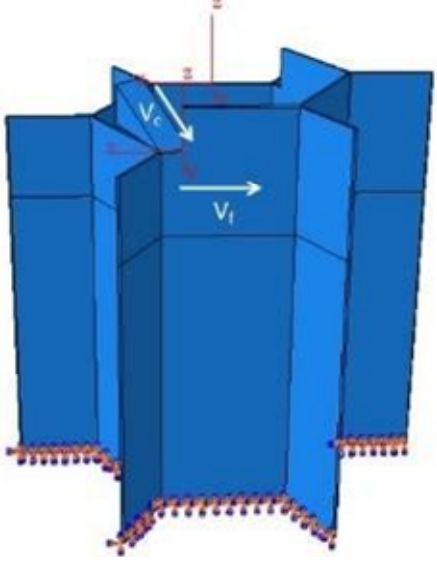

Table 2 Al5052 honeycomb core material parameters

Properties	*Value*
Density (kg/m^3)	2,680
Elastic modulus/GPa	70.3
Poisson's ratio	0.33
Thermal conductivity (W/mk)	137.7
Specific heat J/(kg/k)	930

Source: Mahabunphachai et al. (2010), Morejón et al. (2010)

2.2 Material properties and failure model

The constitutive model of honeycomb core material adopts Johnson-Cook plastic flow model (Cook et al., 1985).

$$\tilde{\sigma} = \left[A + B(\dot{\varepsilon})^n\right]\left[1 + C\ln\left(\frac{\varepsilon}{\varepsilon_0}\right)\right]\left[1 - \left(\frac{T - T_0}{T_m - T_0}\right)^m\right] \tag{1}$$

where $\tilde{\sigma}, \dot{\varepsilon},$ and ε_0 are the equivalent stress, the equivalent plastic strain and reference strain rate; T_0, T_m and T are the room temperature, melting point of materials, and the temperature when the material deforms. A, B, C, m, and n are the strength, harding modulus, strain rate sensiticity, thermal softening index. The parameter settings are shown in Table 3.

Table 3 The Johnson-Cook constant parameter of Al5052

A/MPa	*B/MPa*	*c*	*n*	*m*	T_m/℃	T_0/℃
92.4	132	0.02511	0.25	1	580	20

Source: Qin et al. (2020)

Meanwhile, the Johnson-Cook progressive damage model was used, which takes into account the damage evolution and allows the material to rupture when the damage parameter reaches one. The damage parameter D is shown in equation (2).

$$D = \sum \frac{\Delta\varepsilon}{\varepsilon^f} \tag{2}$$

where $\Delta\varepsilon$ is an increment of the equivalent plastic strain, and ε^f is the equivalent strain to fracture, which bases on strain rate, temperature, pressure and equivalent stress. The expression of ε^f is shown in equation (3):

$$\varepsilon^f = \left[D_1 + D_2\exp\left(D_3\frac{\sigma_m}{\sigma}\right)\right]\left[1 + D_4\ln\left(\frac{\varepsilon}{\varepsilon_0}\right)\right]\left[1 + D_5\left(\frac{T - T_0}{T_m - T_0}\right)\right] \tag{3}$$

where D_1~D_5 are the damage parameters of the material, as shown in Table 4, σ_m is hydrostatic pressure; σ is the Mises equivalent stress.

Table 4 Johnson-Cook damage parameters of Al5052

D1	*D2*	*D3*	*D4*	*D5*
0.306	0.446	–1.72	0.0056	0

Source: Zeng et al. (2015)

3 Experiment design

The honeycomb core material used in this test is Al5052 material, aluminium honeycomb core lattice is positive hexagonal, aperture diameter of 6mm, thickness of single wall of 0.06mm. the workpiece specification is 20*10*10mm. the cutter is a carbide milling cutter with the diameter of 12.7mm, the rake angle of 15°, the clearance angle of 35°, the helix angle of 30°. The test parameters are shown in Table 5.

Table 5 Experimental parameter

Properties	*Value*
Workpiece	Al5052 honeycomb core
Feed speed (mm/min)	240, 480, 720, 960
Cutting speed(m/min)	240, 320, 400
Entrance angle/°	10, 13, 30, 45, 60, 75, 90, 105, 120, 135, 150, 160, 170
Cutting depth/mm	1

In order to verify the accuracy of the simulation model, the honeycomb core is milled on the DMU100 five-axis machining centre. The most commonly used fixing method for processing aluminium honeycomb cores is adopted. Firstly, a clamping plate slightly larger than the workpiece is preset, and the workpiece is bonded to the clamping plate by the adhesive. Secondly, the clamping plate with the workpiece is placed above the dynamometer. Finally, the pressure block is placed above the allowance reserved for the clamping plate, and the clamping plate is fixed on the dynamometer by bolt connection. The milling test platform is set as shown in Figure 3. The cutting force in the X and Y directions is checked by a Kistler 9257B force measuring instrument.

Figure 3 Milling test platform (a) Milling test device, (b) Processing platform schematic diagram

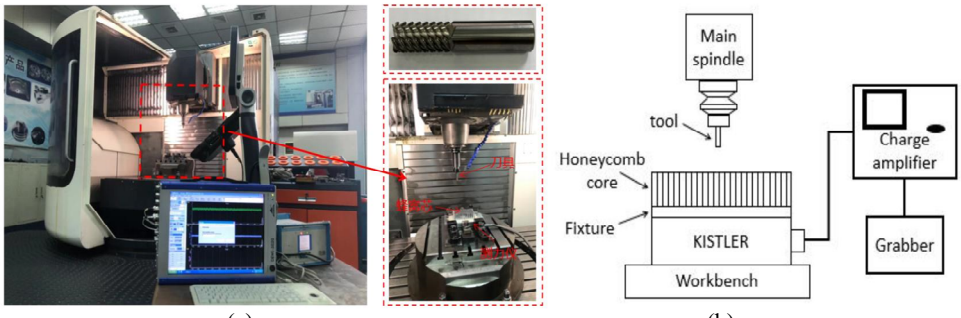

(a) (b)

4 Result and discussion

4.1 Cutting force

Due to the large amplitude of cutting vibration in the initial stage of cutting, the cutting force is unstable. After entering the plastic cutting stage, the cutting force gradually tends to be stable, and the average value of the stable region is taken as the cutting force. The finite element model is a single honeycomb wall cutting, and several honeycomb core walls are involved in the actual machining process. Through the finite element model, the cutting force F is obtained. The $F_{\perp}$ and $F_{\parallel}$ are obtained in the equation (4), and the $F_{\perp}$ and $F_{\parallel}$ are brought into the equation (5) to obtain F_x and F_y. Compared with the experimental data, the specific calculation formula is as follows (Qiu et al., 2016).

$$\begin{cases} F_{\perp} = F\sin\left(\frac{5}{6}\pi - \theta\right) \\ F_{\parallel} = F\cos\left(\frac{5}{6}\pi - \theta\right) \end{cases} \tag{4}$$

where $F_{\perp}$ force perpendicular to the honeycomb wall, $F_{\parallel}$ force parallel to the honeycomb wall, F is the resultant force of X-Y plane.

$$\begin{cases} F_x = H(X)\sum_n \left(-F_{\perp}^n \cos\beta^n - F_{\parallel}^n \sin\beta^n\right) \\ F_y = H(X)\sum_n \left(-F_{\perp}^n \sin\beta^n - F_{\parallel}^n \cos\beta^n\right) \end{cases} \tag{5}$$

where F_x the total cutting force in X direction, F_y the total cutting force in Y direction, n stands for the nth honeycomb wall in the cutting region. When the tool is in contact with the honeycomb wall, $H(X)$ takes 1, and otherwise takes 0. β is the angle between the honeycomb wall and the y direction, as shown in Figure 1.

Figure 4 (a) Model cutting force and (b) test cutting force varying with time (see online version for colours)

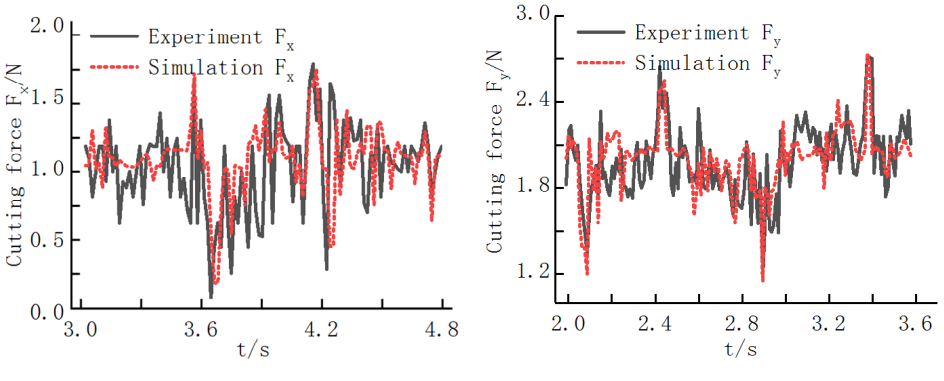

Figure 4 shows the comparison between the simulated and experimental values of cutting force F_x and F_y changing with time. The simulation value of the cutting force has a good

correlation with the experimental value. The reason for the error is that this study assumes that each honeycomb wall in the machining area contributes to the cutting force, but in actual machining, the cutting force is generated only when the tool is in contact with the honeycomb wall.

Figure 5 shows the comparison between the experimental value and the calculated simulation value of the cutting force under different milling parameters. It can be seen from the diagram that the experimental value and the simulation value have the same change trend. When cutting speed = 320 m/min and the feed speed increases from 240 mm/min to 960 mm/min, the extrusion force of the blade on the honeycomb wall is stronger. Therefore, the extrusion force and friction force received by the honeycomb wall increase with the increase of the feed speed, which leads to the increase of the cutting force. The maximum relative error is 10.64%, and the minimum relative error is only 3.79%. When feed speed = 960 mm/min and the cutting speed increases from 240 m/min to 400 m/min, the material removed per revolution decreases, so the cutting force generally decreases, and the overall relative error is less than 15%. The reason for the error is that the established simulation model assumes certain conditions, as well as various factors such as machining chatter and measuring instruments during machining.

Figure 5 Comparison of simulation values and test values under different cutting parameters (a) Vf, (b) Vc (see online version for colours)

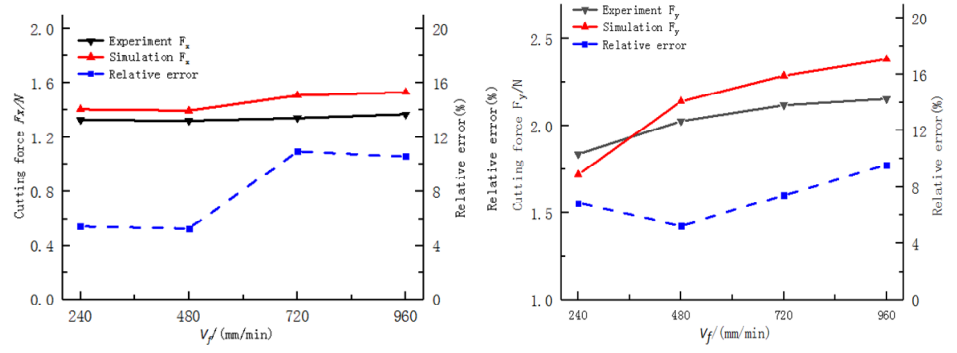

(a)

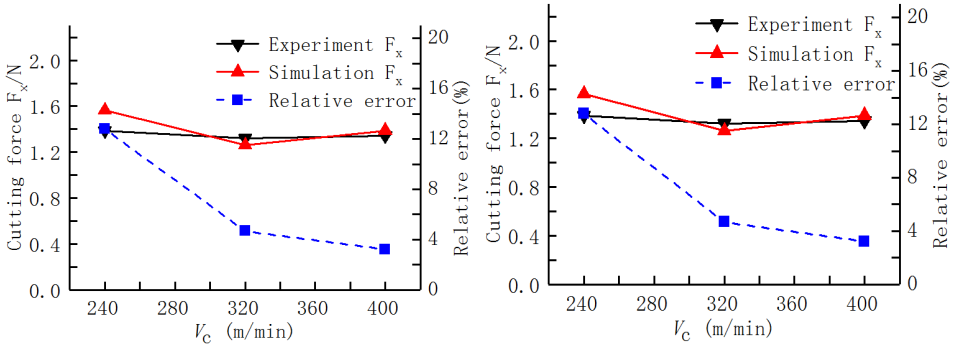

(b)

4.2 Tearing defect analysis

At present, there is no uniform standard for the characterisation of surface tearing defects in macro cutting of honeycomb cores. The lack of honeycomb wall is the manifestation of tearing defects on the machined surface. In this paper, the volume of honeycomb wall loss is selected as the evaluation index of tearing defect degree (Zhang et al., 2022), as shown in Figure 6. In the following, the volume of tearing defect represents the volume of missing honeycomb wall. The volume of tearing defect is equal to the product of the area of the honeycomb wall missing grid on X–Z and the honeycomb wall thickness δ. According to the mesh size, the number of missing meshes in the finite element model after cutting is calculated to obtain the missing mesh area of the honeycomb wall on X–Z.

Figure 6 Characterisation diagram of tearing defect (see online version for colours)

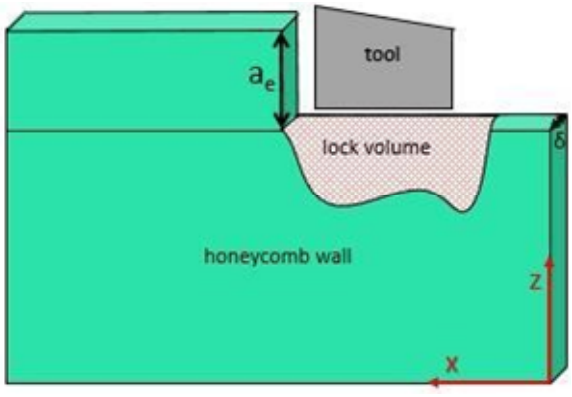

Figure 7 The volume of tearing defects at different entrance angles, (a) the comparison of tearing defects between the simulation and experiment; (b) simulation and An et al. (2019) test comparison (see online version for colours)

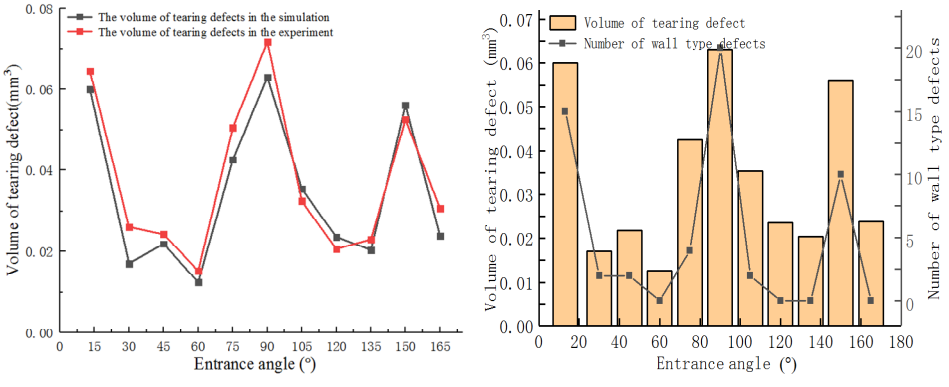

(a) (b)

Jiang (2021) used the number of cracks in the NOMEX honeycomb wall as the evaluation index of tearing defects, but the cracks in the honeycomb wall did not necessarily develop into tearing defects. Compared with the number of cracks on the honeycomb wall, the missing volume of the honeycomb wall can better quantify the

degree of tearing defects. An et al. (2019) analysed the number of wall type defects composed of burrs, honeycomb wall cracks, and honeycomb wall depressions at different entrance angles, burrs are caused by the extrusion and tearing of the material, the honeycomb wall crack is the initial form of the tearing defect, and the honeycomb wall crack is formed by the honeycomb wall depression. Although the wall type defect can not fully represent the tearing defect, it can still be used as the evaluation standard of tearing defect. If the number of wall type defects under a certain entrance angle is more, the tearing defect under the entrance angle is more serious.

Figure 7(a) shows the comparison of tearing defects between the simulation and experiment. Compared with the experimental data of An et al. (2019) as shown in Figure 7(b).

4.3 The influence of entrance angle on tearing defects

When V_c =400 m/min, V_f = 240 mm/min, Figure 8 shows the changes of tearing defect volume and cutting force at different entrance angles. The entrance angle is divided into four regions. The entrance angle at region I is nearly 13°, the entrance angle at region II is nearly 90°, and the entrance angle at region III is nearly 150°, in addition to region IV.

Figure 8 Tearing defects and cutting forces at different entrance angles (see online version for colours)

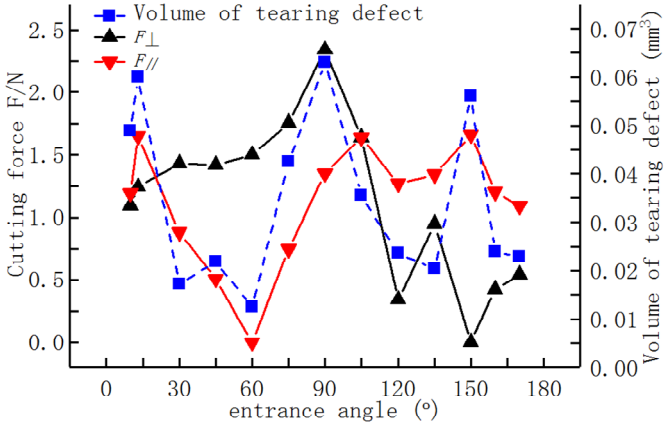

Figure 9 shows the effect of entrance angle on tearing defects. When the entrance angle is in region I and region III, the material removal rate is low and the tearing defect is serious. The reason is that the tool initially only has one point on the edge to participate in the cutting of the corresponding honeycomb wall. As the tool tip gradually cuts into the honeycomb wall, the interaction between the rake face of the tool and the honeycomb wall gradually increases, resulting in large distortion and tearing of the honeycomb wall, and the material is difficult to be removed at one time. At this time, the force $F_{\parallel}$ parallel to the honeycomb wall is the reason for the formation of tearing defects. The larger cutting force in region I leads to plastic deformation of the workpiece material along the cutting direction, and there is no support on the cutting side, so the material cannot be removed, resulting in tearing defects, as shown in Figures 9(a)–9(c). The surface material in region III is removed smoothly, and the larger force $F_{\parallel}$ parallel to the honeycomb wall

leads to the excessive extrusion force of the blade on the honeycomb wall in this region, which means that it is easy to produce excessive tearing defects. When the entrance angle is in region II, the force $F_{\perp}$ perpendicular to the honeycomb wall is the main factor affecting the tearing of the honeycomb wall. The material is removed by a smaller cutting force, but the force $F_{\perp}$ perpendicular to the honeycomb wall reaches its peak, and excessive material is removed, resulting in an increase in the tearing volume of the honeycomb wall and more serious defects, as shown in Figure 9(d). The cutting force of region IV is relatively low, and the load acting on the honeycomb wall is lower than other regions, so the degree of tearing defects in this region is low and the integrity of the machined surface is good. This shows that the entrance angle has a great influence on the tearing defects in regions I–III.

Figure 9 Effect of entrance angle on tear defect (a) θ = 13°, (b) θ = 60°, (c) θ= 75°, (d) θ = 90°, (e) θ = 120°, (f) θ = 150°(see online version for colours)

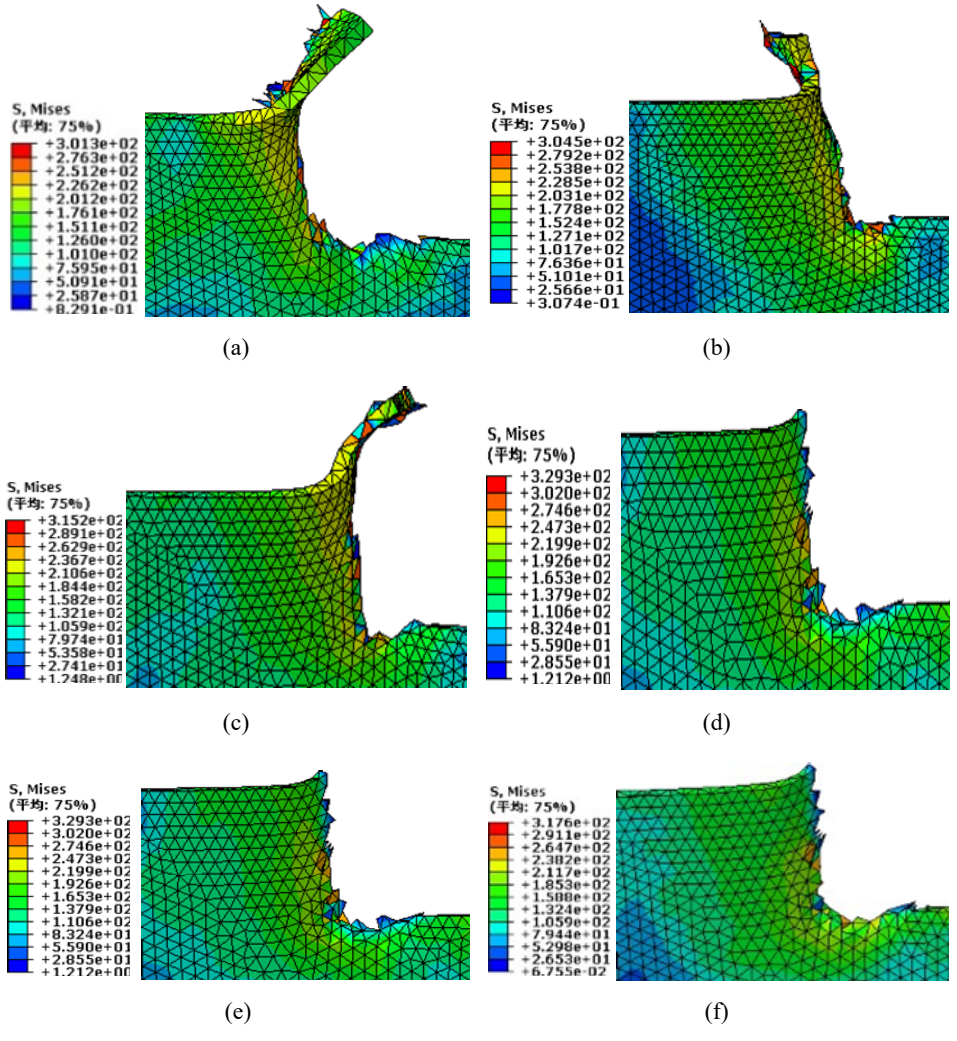

4.4 Effect of feed speed on tearing defects

Figure 10 shows the influence of feed speed on tearing defects and cutting force when θ = 90°, V_c = 320 m/min. The analysis shows that the material can be removed by a small cutting force at this time. When V_f = 960 mm/min, the force $F_\perp$ perpendicular to the honeycomb wall is relatively large. The tool tip cuts into the honeycomb wall, with the feed of the tool, the material on the honeycomb wall that should not be removed is pulled out along the machining direction, resulting in a large tear defect. With the increase of the feed, the force $F_\perp$ perpendicular to the honeycomb wall gradually increases, and the load acting on the honeycomb wall also increases. Therefore, with the increase of feed speed, the volume of tearing defect of honeycomb wall increases. This shows that the size of the tearing defect volume is closely related to the feed speed.

Figure 10 Tearing defects and cutting forces at different feed speeds (see online version for colours)

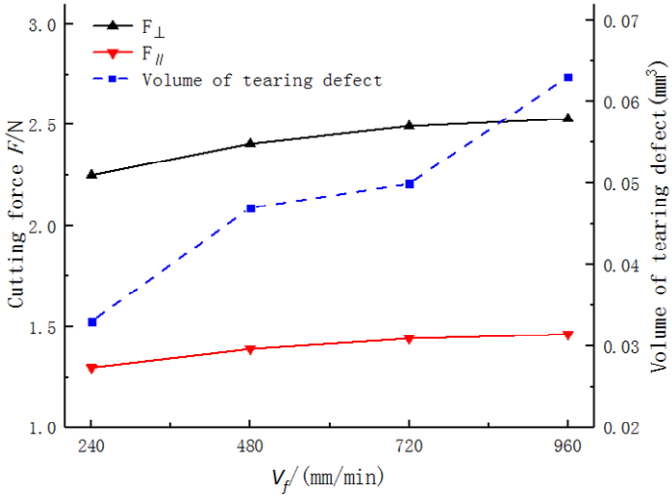

4.5 Effect of cutting speed on tearing defects

Figure 11 shows the influence of cutting speed on tearing defects and cutting force when θ = 90 ° and V_f = 960 mm/min. It can be seen from the diagram that with the increase of cutting speed, the cutting force and the volume of tearing defects gradually decrease. However, the change trend is not significant when the cutting speed is greater than 320 m/min. The reason is that a smaller cutting force can remove the material, and when the cutting speed is 240 m/min, the force $F_\perp$ perpendicular to the honeycomb wall is larger, resulting in a larger load acting on the honeycomb wall and a larger tearing volume of the honeycomb wall. When the cutting speed is more than 320 m/min, litter change in cutting force, so the load acting on the honeycomb wall does not much has change, this is also the reason why the volume of tearing defects does not change much. This shows that when the cutting speed reaches a certain value, the cutting speed has little effect on the tearing defect.

Figure 11 Tearing defects and cutting forces at different cutting speeds (see online version for colours)

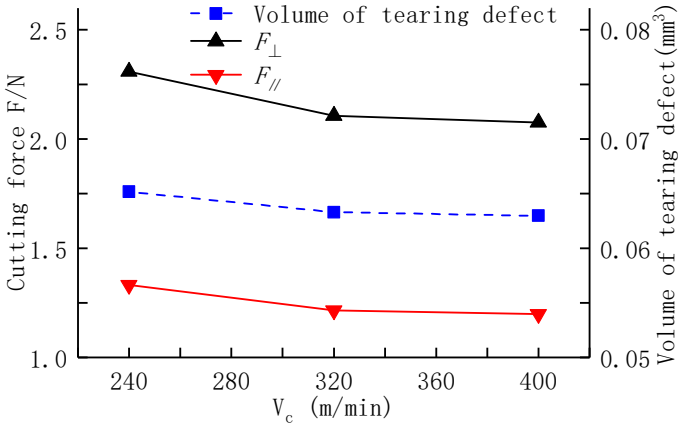

Figure 12 The relationship between the force $F_{\parallel}$ parallel to the honeycomb wall and the tearing defect (see online version for colours)

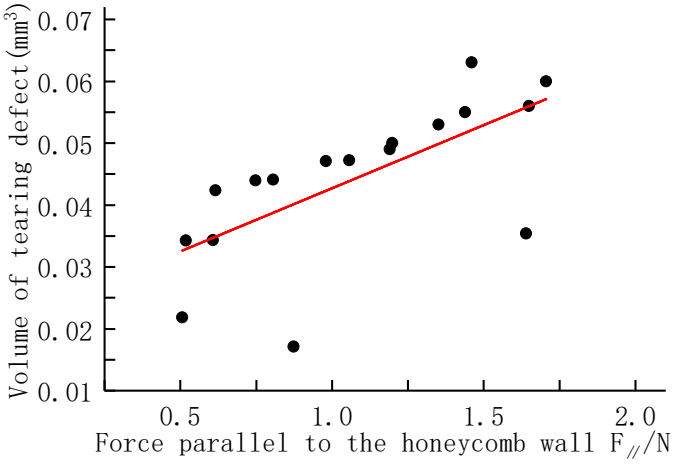

Through the above research, it is found that when the entrance angle is 90° the tear defect volume is 0.063 mm^3, and when the entrance angle is 60°, the tear defect volume is 0.0125 mm^3, and the difference between the two is 0.0505 mm^3. When the feed speed is 960 mm/min, the tear defect volume is 0.06 mm^3, and when the feed speed is 240 mm/min, the tear defect volume is 0.03 mm^3, the difference between the two is 0.033 mm^3. When the cutting speed is 400 m/min, the volume of tearing defect is 0.063 mm^3, and when the cutting speed is 240 m/min, the volume of tearing defect is 0.0652 mm^3, the difference between the two is only 0.0022 mm^3. This shows that the effect on tearing defects follows the entrance angle > feed speed > cutting speed. At the same time, it is found that the change trend of the force $F_{\parallel}$ parallel to the honeycomb wall is similar to that of the tearing defect. The correlation between the two is fitted, and the correlation coefficient r = 0.67071 is obtained, as shown in Figure 12. Therefore, it can

be explained that the tearing defect is positively correlated with the force $F_{\parallel}$ parallel to the honeycomb wall.

5 Conclusions

In this paper, the honeycomb wall cutting model is established. The effects of feed speed, cutting speed and cutting angle on tearing defects and cutting force were discussed by using the model, and the relationship between cutting force and tearing defects was further explored.

1 The cutting model of honeycomb wall was established by ABAQUS. Compared with the experimental data of cutting force, the relative error is less than 15%. Compared with the experimental data, the distribution of tearing defects is generally consistent. It shows that the finite element model is correct and can be used to analyse the tearing defects of aluminium honeycomb core.

2 When the entrance angle is in region I and III, the force $F_{\parallel}$ parallel to the honeycomb wall is the main reason for the formation of tearing defects. When the entrance angle is in region II, the force $F_{\perp}$ perpendicular to the honeycomb wall has a great influence on the tearing defects.

3 It is helpful to reduce the cutting force and improve the processing quality by controlling the change of the entrance angle and selecting the larger cutting speed and the smaller feed speed.

4 The tearing defect is positively correlated with the force $F_{\parallel}$ parallel to the honeycomb wall, and the influence on the tearing defect follows the entrance angle > feed speed > cutting speed.

References

An, Q., Jiaqiang, D., Weiwei, M., Qiu, K. and Chen, M. (2019) 'Experimental and numerical studies on defect characteristics during milling of aluminium honeycomb core', *Journal of Manufacturing Science and Engineering*, Vol. 141, No. 3, DOI:10.1115/1.4041834.

Cook, J. (1985) 'Fracture characteristics of three metals subjected to various strains, strain rates, temperatures and pressures', *Engineering Fracture Mechanics*, Vol. 21, No. 1, DOI:10.1016/0013-7944(85)90052-9.

Hamid, M., Mohammed, N. and Mohamed, J. (2022) 'Surface integrity quantification in machining of aluminium honeycomb structure', *Procedia CIRP*, Vol. 108, pp.693–697, DOI:10.1016/J.PROCIR.2022.03.107.

Jaafar, M., Atlati, S., Makich, H., Nouari, A. and Julliere, B. (2017) 'A 3D FE modeling of machining process of nomex honeycomb core: influence of the cell structure behaviour and specific tool geometry', *Procedia Cirp*., Vol. 58, pp.505–510, DOI:10.1016/j.procir.2017.03.255.

Jiang, J. (2021) *Nomex Honeycomb Cutting Surface Tear Generation and Inhibition*, Shandong University, DOI:10.27272/d.cnki.gshdu..004210.

Jiang, J. and Liu, Z. (2021) 'Formation mechanism of tearing defects in machining Nomex honeycomb core', *The International Journal of Advanced Manufacturing Technology*, Vol. 112, No. 11, pp.1–10, DOI:10.1007/S00170-021-06603- 8.

Mahabunphachai, S. and Koc, M. (2010) 'Investigations on forming of aluminium 5052 and 6061 sheet alloys at warm temperatures', *Materials and Design*, Vol. 31, No. 5, pp.2422–2422, DOI:10.1016/j.matdes..11.053.

Morejón, P., Morales, F., Rodríguez, Y., Crespo, A., Cedre, E. and Scott, A. (2010) 'Modelling using finite element analysis of stress and strain in gas metal arc welding on 5052 H32 aluminium alloy', *Welding International*, Vol. 24, No. 7, pp.509–517, DOI:10.1080/0950711 0902844600.

Qin, Q., Chen, S., Li, K., Jiang, M., Cui, T. and Zhang, J. (2020) 'Structural impact damage of metal honeycomb sandwich plates', *Composite Structures*, Vol. 252, DOI: 10.1016/j. compstruct.2020.112719.

Qiu, K., Ming, W., Shen, L., An, Q. and Chen, M. (2016) 'Study on the cutting force in machining of aluminium honeycomb core material', *Composite Structures*, Vol. 2017, p.164, DOI:10.1016/j.compstruct..Vol.12, pp.060.

Qiu, K.X. (2017) *Physical Modeling and Technological Research of Aluminium Honeycomb Core Material Cutting Process*, Shanghai Jiao Tong University, Shanghai.

Shi, L., Wang, C., Chen, J., Guo, G., Huang, W., An, Q., Ming, W. and Chen, M. (2022) 'Material removal mechanism and damage behavior in high speedmilling of superalloy honeycomb core', *Journal of Mechanical Engineering*, Vol. 58, No. 23, pp.284–295.

Sun, J., Dong, Z., Wan, G.Y., Liu, J., Qin, Y. and Kang, R. (2017) 'Experimental study on ultrasonic cutting aluminium honeycomb', *Journal of Mechanical Engineering*, Vol. 53, No. 19, p.8, DOI:10.3901/JME.2017.19.128.

Tarik, Z., Eddine, S.J., Mohammed, N., Merzouki, S., Elmiloud, C., Hamid, M. and Najim, S. (2022a) 'Modeling machining of aluminium honeycomb structure', *The International Journal of Advanced Manufacturing Technology*, Vol. 123, Nos. 7–8, pp.2481–2500, DOI:10.1007/ S00170-022-10350-9.

Tarik, Z., Mohammed, N., Eddine, J.S. et al. (2022b) 'Optimization of the milling process for aluminium honeycomb structures', *The International Journal of Advanced Manufacturing Technology*, Vol. 119, Nos. 7–8, DOI:10.1007/S00170- 021-08495-0.

Wang, F., Liu, J., Li, L. and Qin, S. (2017) 'Green machining of aluminium honeycomb treat ed using ice fixation in cryogenic', *The International Journal of Advanced Manufacturing Technology*, Vol. 92, Nos. 1–4, pp.943–952, DOI:10.1007/s00 170-017-0181-9.

Wang, L., Duan, C., Li, C., Chang, B. and Zhang, T. (2021) 'Study on deformation of aluminum honeycomb core wall in high speed milling', *Tool Engineering*, Vol. 55, No. 9, pp.42–46.

Wang, Y., Gan, Y., Liu, H., Wang, J. and Liu, K. (2020a) 'Surface quality improvement in machining an aluminium honeycomb by ice fixation', *Journal of Mechanic al Engineering*, Vol. 33, No. 1, pp.20–20, DOI:10.1186/s10033-020-00439- 1.

Wang, Z., Wang, Z, Zhou, X., Liu, J., Li, J. and Zhu, L. (2020b) 'Development status of honeycomb sandwich structure and forming technology for civil aircraft', *Fiber Composites*, Vol. 37, No.03, pp.87–90, DOI:10.3969/j.issn.1003-6423. 2020.03.018.

Zeng, R., Ma, F., Huang, L. and Li, J. (2015) 'Investigation on spinnability of profiled power spinning of aluminium alloy', *The International Journal of Advanced Manufacturing Technology*, Vol. 80, Nos. 1–4, DOI:10.1007/s00170-015-7025-2.

Zhang, T., Duan, C., Chang, B., Li, C. and Wang, L. (2022) 'Effect of aluminium honey comb core processing defects on honeycomb flat pressing performance', *Combined Machine Tool and Automatic Processing Technology*, Vol. 2022, No. 2, pp.133–136, DOI:10.13462/j.cnki. mmtamt..02.031.

Zhang, T.X. (2021) *Milling Defects of Aluminium Honeycomb Core and Their Effects on Mechanical Properties of Sandwich Structures*, Dalian University of Technology, Dalian, DOI:10.26991/d.cnki.gdllu.2021.000787.